JOURNAL OF GEOPHYSICAL RESEARCH, VOL. 106, NO. C10, PAGES 22,143–22,158, OCTOBER 15, 2001

Mean transport and seasonal cycle of the Kuroshio east of Taiwan with comparison to the Florida Current

Thomas N. Lee,[1] William E. Johns,[1] Cho-Teng Liu,[2] Dongxiao Zhang,[1] Rainer Zantopp,[1] and Yih Yang[2]

Abstract. Moored observations of Kuroshio current structure and transport variability were made across the channel between northeast Taiwan and the Ryukyu Islands at 24°N from September 19, 1994, to May 27, 1996. This was a cooperative effort between the United States and Taiwan. The moored array was designated PCM-1, for the World Ocean Circulation Experiment (WOCE) transport resolving array. The dominant current and transport variability occurred on 100-day timescales and is shown by *Zhang et al.* [2001] to be caused by warm mesoscale eddys merging with the Kuroshio south of the array causing offshore meandering and flow splitting around the Ryukyu Islands. An annual transport cycle could not be resolved from our 20-month moored record because of aliasing from the 100-day period events. Sea level difference data were used to extend the transport time series to 7 years giving a variation in the range of the annual transport cycle of 4–10 Sv, with a mean range closer to 4 Sv. The seasonal maximum of 24 Sv occurred in the summer and the seasonal minimum of 20 Sv occurred in the fall. A weaker secondary maximum also occurred in the winter. The cycle of Kuroshio transport appears to result from a combination of local along-channel wind forcing and Sverdrup forcing over the Philippine Sea. Our estimate of the mean transport of the Kuroshio at the entrance to the East China Sea from the moored array is 21.5 ± 2.5 Sv. The mean transpacific balance of meridional flows forced by winds and thermohaline processes at this latitude requires an additional mean northward flow of 12 Sv with an annual cycle of ±8 Sv along the eastern boundary of the Ryukyu Islands. The mean transport and annual cycle of the Kuroshio were found to be in reasonable agreement with basin-scale wind-forced models. Remarkable similarities are shown to exist between the mean western boundary currents and their seasonal cycles in the Atlantic (Florida Current and Antilles Current) and Pacific (Kuroshio and boundary current east of Ryukyu Island chain) at the same latitude. However, detailed comparison shows that the mean Kuroshio is weaker and more surface intensified than the mean Florida Current, while the Kuroshio transport variability is significantly larger.

1. Introduction

The Kuroshio in the northwest Pacific and its counterpart, the Gulf Stream in the northwest Atlantic, are the two major western boundary currents in the Northern Hemisphere and important links in the global climate system. However, unlike the Gulf Stream, which has been intensively studied over the past several decades, many aspects of the Kuroshio remain relatively obscure. Knowledge of Kuroshio flow was previously based primarily on snapshots from hydrographic sections with inherent difficulties associated with referencing the geostrophic currents and aliasing by meanders and eddies. Only recently have moored measurements of the Kuroshio transport been obtained (this study and off the southeast coast of Japan by *Imawaki et al.* [2001]).

The Kuroshio in the East China Sea (ECS) is somewhat analogous to the Florida Current in the Straits of Florida in that both western boundary currents are separated from ocean basin interior processes by island chains, the Ryukyus and Bahamas, respectively. However, whereas a stable mean flow of 31.7 ± 3 Sv (10^6 m^3/s) has been well established for the Florida Current from a long history of intensive studies [*Schmitz and Richardson*, 1968; *Niiler and Richardson*, 1973; *Molinari et al.*, 1985; *Leaman et al.*, 1987; *Schott et al.*, 1988; *Schmitz and Richardson*, 1991], estimates of the mean Kuroshio transport in the ECS vary by as much as 12 Sv from ~21 to 33 Sv, inferred mainly from indirect methods [*Nitani*, 1972; *Guan*, 1981; *Roemmich and McCallister*, 1989; *Bryden et al.*, 1991; *Bingham and Talley*, 1991; *Ichikawa and Beardsley*, 1993]. Both current systems are the primary ocean conduits for the poleward transport of heat from the tropics to northern latitudes. However, because of the lack of deep water formation in the North Pacific the meridional heat flux is primarily contained in the shallow circulation of the wind-driven subtropical gyre [*Roemmich and McCallister*, 1989; *Bryden et al.*, 1991]. The net meridional heat flux across 24°N is estimated at 0.76 ± 0.3 PW (1 PW = 10^{15} W) poleward [*Roemmich and McCallister*, 1989], with approximately half due to an Ekman overturning cell in the upper 700 m and half due to the horizontal circulation of the subtropical gyre, also concentrated in the upper

[1]Rosenstiel School of Marine and Atmospheric Science, University of Miami, Miami, Florida, USA.
[2]Institute of Oceanography, National Taiwan University, Taipei, Taiwan.

Paper number 2000JC000535.
0148-0227/01/2000JC000535$09.00

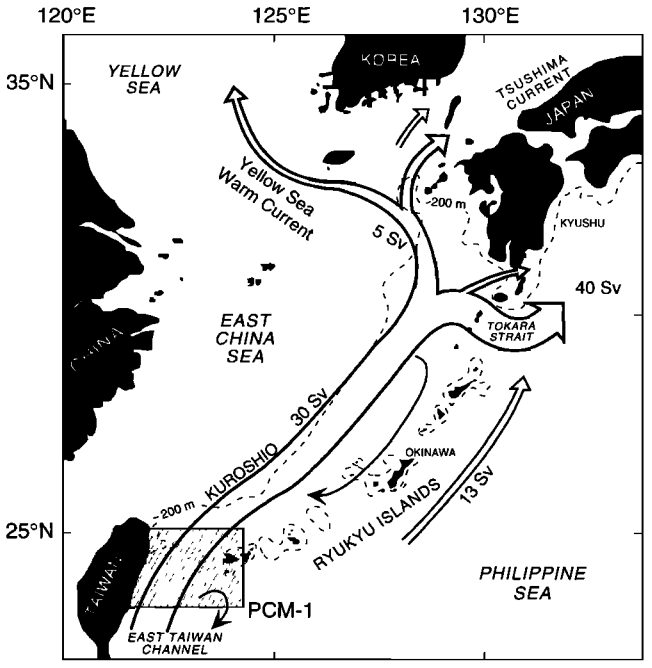

Figure 1. Schematic of the western boundary currents and mean transports in the vicinity of the East China Sea. The study region containing the PCM-1 transport array site is highlighted.

700 m [*Bryden et al.*, 1991]. One of the largest uncertainties in estimates of the net heat flux is the poorly resolved mean flow of the Kuroshio. In a similar fashion, uncertainties regarding seasonal and interannual variability of the heat flux across 24°N is also related to the uncertainties of Kuroshio transport changes on these timescales.

A schematic presentation of the current patterns in this region from *Nitani* [1972] is shown in Figure 1 with previous estimates of the mean volume transports from hydrographic data. According to this schematic and other estimates the subtropical gyre splits just south of the Ryukyus with ~20–30 Sv flowing northward through the East Taiwan Channel (ETC) between northeast Taiwan and the Ryukyu Islands on the average [*Nitani*, 1972; *Worthington and Kawai*, 1972; *Roemmich and McCallister*, 1989; *Bryden et al.*, 1991; *Ichikawa and Beardsley*, 1993] and part turning east into a subtropical counter current, then recirculating back into the North Equatorial Current and Kuroshio [*Nitani*, 1972; *Hasunuma and Yoshida*, 1978; *White and Hasunuma*, 1980]. North of the ETC the Kuroshio tends to follow the eastern edge of the continental shelf in the East China Sea, then exiting the East China Sea through the Tokara Strait. A small portion of the Kuroshio is believed to branch northwestward over the northern part of the East China Sea and form the Tsushima Current flowing north on the west side of Japan and the Yellow Sea Warm Current between Korea and China [*Nitani*, 1972; *Guan*, 1981]. The mean transport of the Kuroshio has been observed to increase significantly after exiting the ECS through the Tokara Strait [*Nitani*, 1972; *Worthington and Kawai*, 1972; *Imawaki et al.*, 2001], which indicates that a net northward flow must occur east of the Ryukyu Islands. Northward flow has been observed in sections east of Okinawa that range from 4 Sv [*Bryden et al.*, 1991] to 26 Sv [*Worthington and Kawai*, 1972].

Seasonal variation of Kuroshio transport at the Okinawa section analyzed by *Guan* [1981] was shown to have a semiannual period with maximum flow in the spring and late summer and minimum in the early summer and fall. The seasonal range in transport was ~7 Sv, with a maximum of 25 Sv in April and a minimum of 18 Sv in September. Guan also found that the seasonally averaged transport was linearly correlated to the seasonally averaged wind stress curl near Hawaii. *Qiu and Lukas* [1996] used a reduced gravity model of the North Pacific from 5°S to 38°N forced with 32 years of Florida State University (FSU) monthly winds and found a significant annual cycle of Kuroshio transport at 20°N with a maximum of 30 Sv in the spring and a minimum of 19 Sv in the fall that matches Guan's observational result. Monthly averages of *Kawabe*'s [1988] 19-year record of sea level differences at Tokara Strait also show a significant seasonal variation with a maximum in summer and a minimum in fall. Kawabe's analysis shows considerable year-to-year variability in the seasonal cycle, but there is normally a maximum around July and a distinct minimum in the fall. Kawabe estimates the annual transport change from his sea level differences to be ~6 Sv on the average, which is also close to the mean annual transport change of the Florida Current. However, *Ichikawa and Beardsley* [1993] estimate a 20–30 Sv annual change in Kuroshio transport in the East China Sea from their 3 years of hydrographic data, with a maximum in the summer.

Many of the circulation features discussed above for the North Pacific are comparable to analogous circulation patterns in the western boundary region of the subtropical gyre in the North Atlantic, where the Florida Current flows between the Florida coast and the Bahamas Islands and joins the Gulf Stream recirculation, north of the Bahamas, in the area of the Blake Plateau [*Olson et al.*, 1984; *Lee et al.*, 1985; *Schott et al.*, 1988; *Lee et al.*, 1990, 1996]. There is a remarkable similarity in the annual sea level and transport cycle of the Kuroshio in the ECS to that of the Florida Current [*Molinari et al.*, 1985; *Lee and Williams*, 1988; *Schott et al.*, 1988]. Also, the northward flow pattern off the Ryukyus appears similar to the Gulf Stream recirculation that occurs off the Bahamas [*Olson et al.*, 1984; *Lee et al.*, 1990, 1996].

In this paper we present results from the World Ocean Circulation Experiment (WOCE) PCM-1 moored current meter array deployed across the Kuroshio between northeast Taiwan and the Ryukyu Islands from September 1994 to May 1996. In previous papers based on these data we presented the detailed methodologies of PCM-1 transport derivation [*Johns et al.*, 2001], which are expected to have broad applications in other settings. The structure and modes of Kuroshio variability on timescales of days to several months were described by *Zhang et al.* [2001]. Efforts to establish sea level monitoring of the Kuroshio transport variability at the entrance to the ECS were also derived by *Yang et al.* [2001] and *Johns et al.* [2001]. Here we first describe the observed low-frequency flow variability to show the influence of strong 100-day period mesocale processes that can alias season transport cycles. However, our primary focus is on the mean transport and seasonal cycle of the Kuroshio at this location and implications for the gyre structure in the North Pacific due to wind and thermohaline forcing. We also compare results with available model simulations, and a comparison is made with the mean and seasonal cycles of western boundary currents in the north Atlantic, the Florida Current, and the Antilles Current. We further compare the influence of mesoscale eddies on boundary current variability in both oceans.

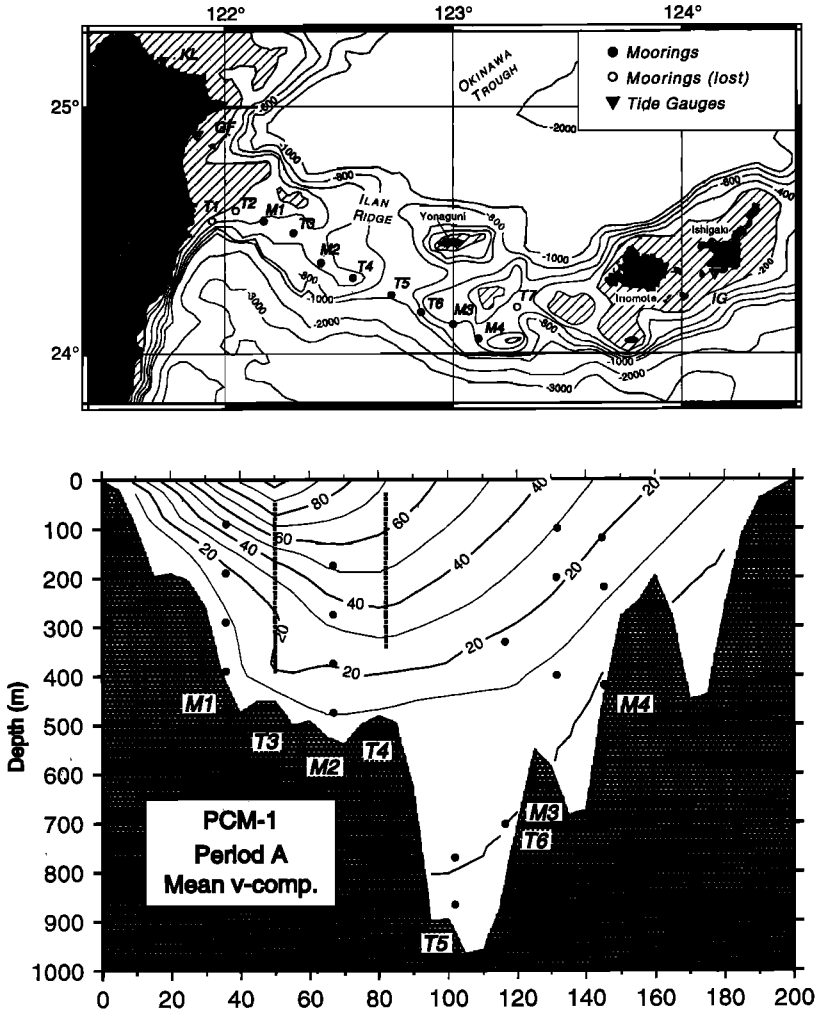

Figure 2. The PCM-1 transport resolving moored current meter array. University of Miami moorings are M1–M4 and National Taiwan University moorings are T3–T6. (a) Mooring and CTD/ADCP station locations on the topography of the Suao Ridge. Also shown are the tide gauge locations at Suao (SA), Geng Fung (GF), Keelung (KL), and Ishigaki Island (IG). (b) Instrumentation configuration superimposed on mean downstream flow field determined from moored current data from period A (September 1995 to May 1996).

2. Observations

The PCM-1 array consisted of 11 current meter moorings deployed from September 19, 1994, to May 27, 1996, along the Ilan Ridge that extends from northeast Taiwan to the Ryukyu Islands (Figure 2). The array instrument configuration is shown in Figure 2b superimposed on the mean downstream flow field derived from the moored current measurements. Details concerning instrument configuration, data recovery, and first order statistics are given by *Johns et al.* [2001]. Mooring and instrument locations, as well as instrument types and measurement periods, are given in Table 1. The array was designed with a 16-km average separation between moorings to resolve the instantaneous transport through the section to about ±2 Sv. This level of uncertainty was believed achievable based on experience with similar arrays in the Florida Current [*Schott et al.*, 1988]. Sea level variations across the ETC were obtained from tide gauges deployed in Geng Fung and Keelung harbors (GF and KL, respectively, in Figure 2a) and a Japanese tide gauge located on Ishigaki Island (IG in Figure 2a). Sea level gauges and dynamic height moorings are shown to be well suited as long-term transport monitoring tools by *Johns et al.* [2001], *Yang et al.* [2001], and this paper.

For direct estimates of transports from the current meter array a gridded cross section of downstream currents (v) through the ETC was computed at 12-hour intervals by the following steps: (1) extrapolation of v to zero at the bottom from the deepest instrument at each mooring; (2) extrapolation of v to the surface from the upper current meter or acoustic Doppler current profiler (ADCP) bin using the vertical shear from below at that time; (3) interpolation of depth corrected v component profiles between instruments on each mooring using a shape-preserving cubic spline fit [*Akima*, 1970]; (4) linear interpolation between moorings; and (5) extrapolation of v to zero at the sides of the channel. These gridded v component cross section fields were then used to derive volume transport time series by zonal integration across the array from the shallow Taiwan shelf to the Ryukyu Islands. For a more detailed explanation of the methods used to derive the gridded velocity fields and to compute transports the reader is referred to *Johns et al.* [2001]. Horizontal currents

Table 1. Mooring Locations and Instrument Depths and Types for PCM-1 Array Deployed East of Taiwan Between September 18, 1994, and May 28, 1996

Mooring ID	Latitude, Longitude	Water Depth, m	Instrument Depth, m	Instrument Type[a]	Duration (yyyymmdd)	Record Length, days
M1	24°32.25'N, 122°10.19'E	464	65	SBE16	Sept. 18, 1994, to Oct. 9, 1995	387
			315[b]		Oct. 10, 1995, to May 28, 1996	232
			90	AACM	Sept. 18, 1994, to Oct. 9, 1995	387
			285[b]		Oct. 10, 1995, to Jan. 12, 1996	95
			140	TSKA	Sept. 18, 1994, to Oct. 9, 1995	387
			240[b]		Oct. 10, 1995, to May 28, 1996	232
			190	VACM	Sept. 18, 1994, to May 28, 1996	619
			250	SBE16	Sept. 18, 1994, to May 28, 1996	619
			300	VACM	Sept. 18, 1994, to May 28, 1996	619
			400	VACM	Sept. 18, 1994, to Nov. 28, 1994	72
T3	24°29.10'N, 122°17.75'E	452	50–390	ADCP	Sept. 18, 1994, to May 22, 1995	247
			415	SBE16	Sept. 19, 1994, to Oct. 8, 1995	385
			30–390	ADCP	Oct. 9, 1995, to May 13, 1996	216
M2	24°22.39'N, 122°25.1'E	538	175	AACM	Sept. 18, 1994, to Aug. 3, 1995	320
			355[b]		Aug. 4, 1995, to May 28, 1996	298
			275	VACM	Sept. 18, 1994, to May 28, 1996	618
			375	VACM	Sept. 18, 1994, to May 28, 1996	618
			475	VACM	Sept. 18, 1994, to May 28, 1996	618
T4	24°18.82'N, 122°33.58'E	477	30–340	ADCP	Sept. 19, 1994, to May 5, 1995	228
			365	SBE16	Sept. 19, 1994, to May 5, 1995	228
			397	SBE16	May 6, 1995, to March 13, 1996	312
T5	24°14.14'N, 122°43.85'E	950	371	SBE16	Sept. 18, 1994, to Oct. 8, 1995	335
			867	AACM	Sept. 18, 1994, to June 30, 1995	286
			379	SBE16	Oct. 14, 1995, to May 27, 1996	226
			573	AACM	Oct. 14, 1995, to May 27, 1996	226
			771	AACM	Oct. 14, 1995, to May 27, 1996	226
			927	TSKA	Oct. 14, 1995, to May 27, 1996	226
T6	24°10.08'N, 122°51.42'E	830	703	AACM	Sept. 18, 1994, to Jan. 23, 1995	128
					Feb. 11, 1995, to May 23, 1995	102
			332	AACM	Oct. 14, 1995, to May 27, 1996	226
			611	AACM	Oct. 14, 1995, to May 27, 1996	226
			813	TSKA	Oct. 14, 1995, to May 27, 1996	226
M3	24°07.33'N, 122°59.9'E	595	75	SBE16	Sept. 19, 1994, to May 27, 1996	617
			100	AACM	Sept. 19, 1994, to March 10, 1996	539
			150	TSKA	Sept. 19, 1994, to May 27, 1996	617
			200	VACM	Sept. 19, 1994, to Dec. 5, 1995	445
			250	SBE16	Sept. 19, 1994, to May 27, 1996	617
			400	VACM	Sept. 19, 1994, to May 27, 1996	617
			594	SBE16	Sept. 19, 1994, to May 27, 1996	617
M4	24°03.44'N, 123°06.86'E	484	95	SBE16	Sept. 19, 1994, to May 27, 1996	617
			120	AACM	Sept. 19, 1994, to Oct. 9, 1995	386
			220	VACM	Sept. 19, 1994, to May 27, 1996	617
			270	SBE16	Sept. 19, 1994, to May 27, 1996	617
			345	TSKA	Sept. 19, 1994, to May 27, 1996	617
			420	VACM	Sept. 19, 1994, to May 27, 1996	617
			483	SBE16	Sept. 19, 1994, to May 27, 1996	617

[a]Instrument types are AACM, Aanderaa current meter; VACM, vector-averaging current meter; ADCP, acoustic Doppler current profiler; SBE16, SeaBird CTD; and TSKA, temperature logger.

[b]Instrument depth is after top float and current meter broke off. See text for further details.

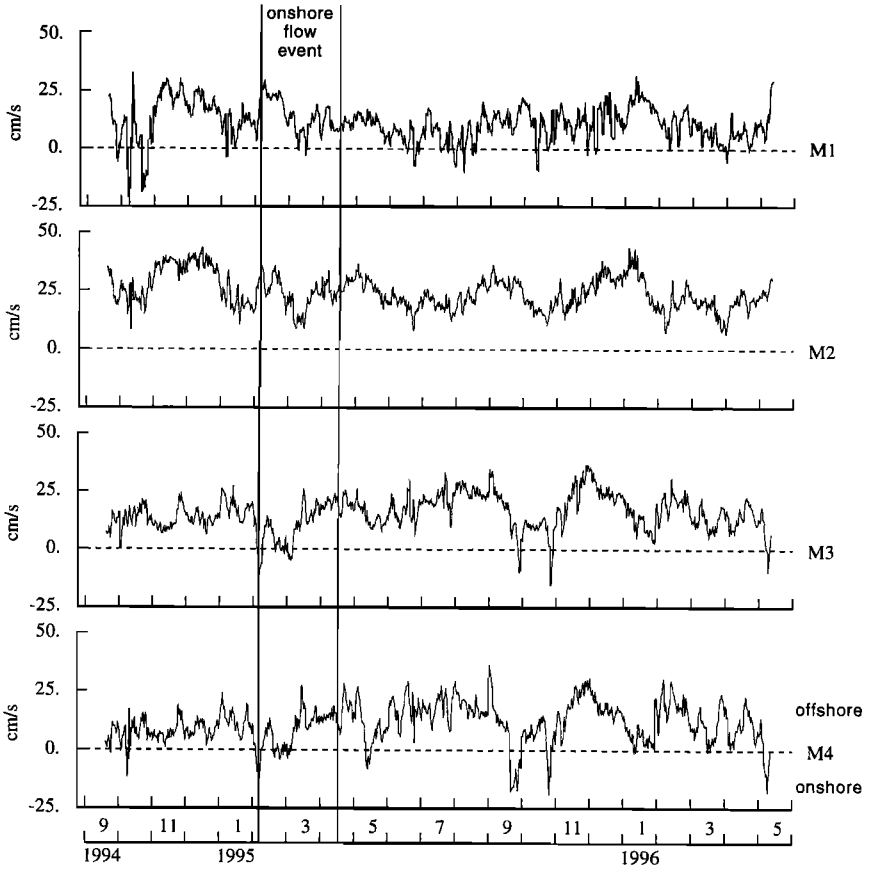

Figure 3a. Subtidal time series of vertically averaged downstream currents (v components) from moorings M1–M4. Vertical event lines highlight the onshore flow event of February and March 1995.

described in this paper have been rotated by 30° so that v is downstream and perpendicular to the alignment of the array, u is positive toward 120°, and v is positive toward 30°.

3. Results

3.1. Mean Flow Structure and Variability

The mean structure of the downstream flow is shown in Figure 2b together with the instrument configuration. Mean flows reach speeds of 100 cm/s in a surface intensified axis located on the western side of the channel near the T3 site. Maximum mean horizontal (cyclonic) and vertical shears are also located on the western side of the channel, similar to the structure of the mean Florida Current. Standard deviations of the downstream and cross-stream flows are typically about the same magnitude and were either less than or equal to the mean flows at all instrument sites [*Johns et al.*, 2001].

Time series of vertically averaged current components over the entire water column at mooring sites M1–M4 and temperature at 300 m are shown in Figures 3a, 3b, and 3c. The vertically averaged currents are shown to condense the visual display since the subtidal variations are for the most part highly coherent and in phase over the vertical extent of the measurements. As shown in Figure 2b, moorings M1 and M2 bracket the mean position of the Kuroshio axis, and M3 and M4 were located on the eastern side of the channel. The magnitude of the downstream vertical averaged currents were similar at M1, M3, and M4 but somewhat larger at M2, indicating a closer location to the axis on the mean. However, the amplitude of the downstream current fluctuations were similar at all moorings. The cross-stream current fluctuations were much larger on the eastern side of the channel than on the west and also comparable to or larger than the downstream current variations.

Spectral analysis shows the current variations to have three dominant energy peaks centered within period bands of 70–120, 30–40, and 12–20 days (Figure 4). Phase relationships between mooring sites indicate that downstream current fluctuations tend to be out of phase on the eastern and western sides of the channel, which is suggestive of horizontal meandering motions of the current axis. *Zhang et al.* [2001] used time domain empirical orthogonal function (EOF) analysis of the combined velocity and temperature fields to show that there are two dominant modes that together explain ~60% of the total variance. The first EOF mode explains 34% of the variance and represents a combined transport/meandering mode with a period of 100 days. The second EOF is characteristic of a meandering mode for fluctuations in the 30- to 40-day period band as indicated by out-of-phase variation of the downstream velocity on either side of the current axis, with temperature fluctuations being in-phase (out-of-phase) with velocity fluctuations on the cyclonic (anticyclonic) sides.

The most significant transport events in the Kuroshio tend to be associated with large-scale meandering of the current axis on the 100-day timescale. For example, hydrographic section data during the period of PCM-1 show that the Kuroshio meandered offshore during mid-March 1995 such that the axis was located on the eastern side of the channel (Figure 5a).

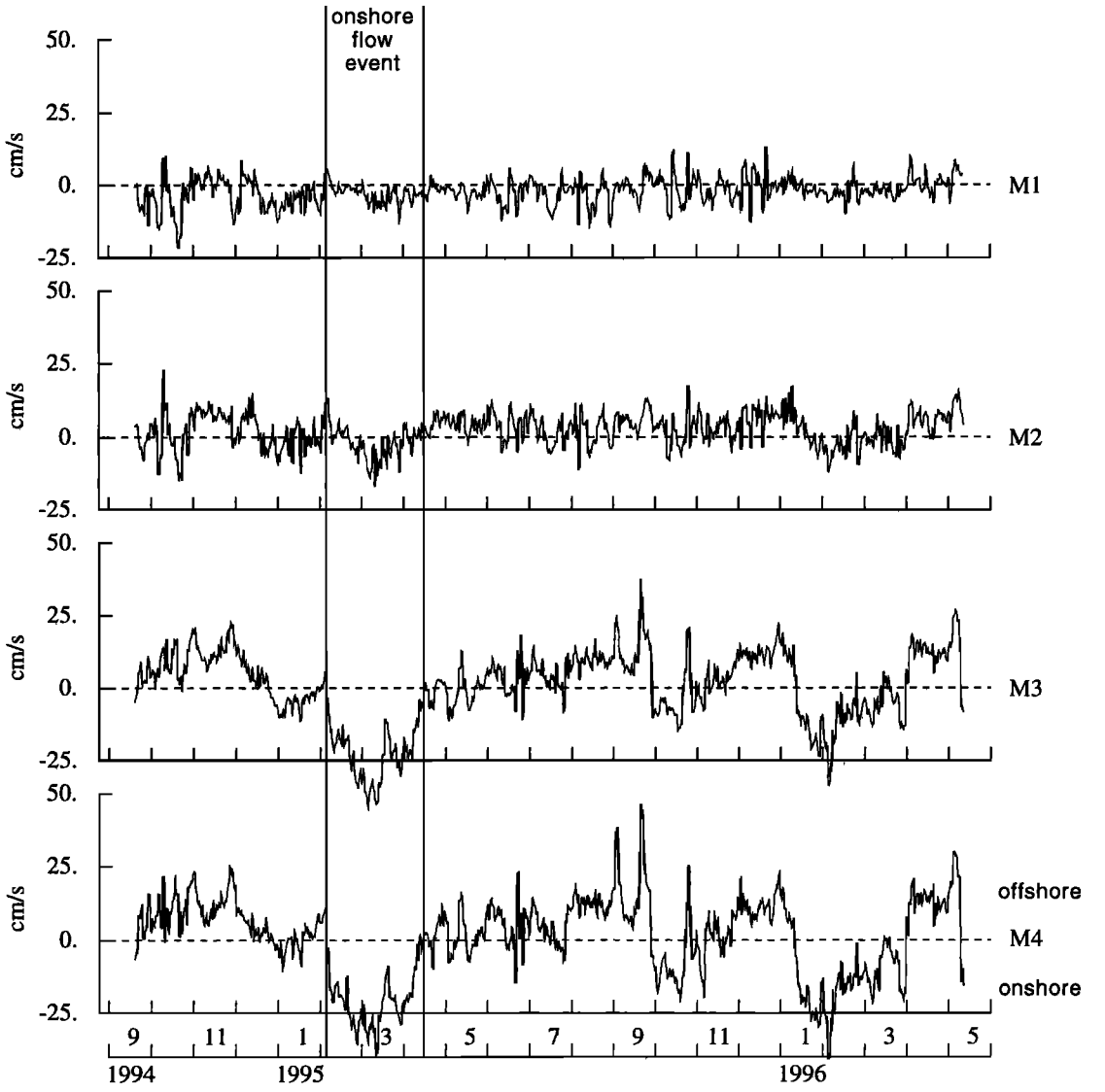

Figure 3b. Subtidal time series of vertically averaged cross-stream currents (u components) from moorings M1–M4.

Within 2 months the jet had meandered back near the coast of Taiwan (Figure 5b). Our moored current data show that this offshore shift of the axis was preceded by strong onshore (westward) vertically averaged flow and decreased temperatures on the eastern side of the channel that began in early February and continued through mid-April (Figures 3b and 3c). Vertically averaged onshore flows maintained speeds of ~50 cm/s at M3 and M4 for nearly 1 month in late February and early March. This onshore flow event appeared later in a much weaker state at the western side of the channel in late February. Downstream flows were near zero at the eastern sites during the strongest part of the onshore flow event and then increased downstream as the axis shifted offshore in mid March (Figure 3a). On the western side of the channel the downstream flow increased through February during the strong onshore flow event then decreased as the axis shifted toward the east in March (Figure 3a). The opposite occurred when the axis shifted back onshore in May 1995; that is, cross-channel flow and temperature increased across the entire channel, while downstream flow increased on the western side and decreased on the eastern side. At least five and possibly six such sequences of events occurred over the total 20-month measurement period giving an average of one event every 100 to 120 days. *Zhang et al.* [2001] used model results and satellite altimeter data to show that these events result from the propagation of warm anticyclonic eddies from the interior into the western boundary where they cause meanders of the Kuroshio and are advected northward with the meander into the ETC. Their average periodicity is ~100 days.

3.2. Volume Transport

Volume transport time series derived from the subtidal gridded downstream velocity fields are shown in Figure 6. Volume transports through the ETC ranged from a minimum of 11 Sv to a maximum of 36 Sv. Spectra of the transport time series show the dominant timescale of variability to occur in the 70- to 120-day period band, but there is also significant variability at periods of 30–40 days and 12–20 days (Figure 7) as previously shown in the current and temperature time series (Figures 3 and 4). Minimum transport events occurred with increased cooling and onshore flow, indicative of offshore meandering of the current axis.

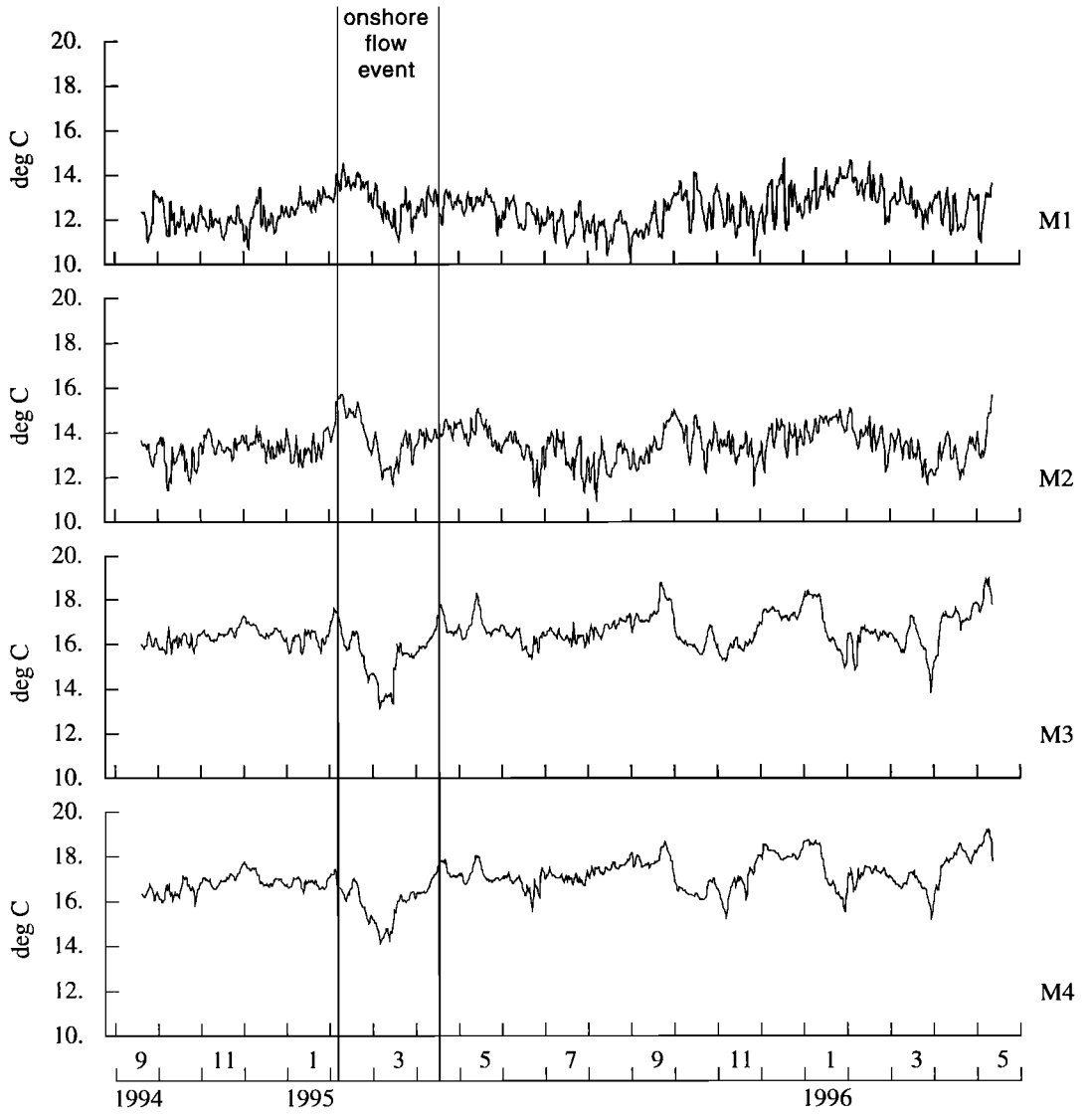

Figure 3c. Subtidal time series of temperature interpolated at 300 m at moorings M1–M4.

The record average transport was 21.5 Sv with a standard deviation of 4.1 Sv. The uncertainty of the transport derivation is ±2.5 Sv as determined by *Johns et al.* [2001] from standard and bias errors. In the ECS a 10-year mean estimate of Kuroshio transport of 25.5 Sv was made by *Fujiwara et al.* [1987] from geostrophic current data on a section west of Okinawa. In the ETC, shipboard-derived geostrophic transports referenced to the bottom between 1990 and 1995 were found to range from 8.5 to 16 Sv, with a mean of only 13.5 Sv, indicating that a significant barotropic transport must also be accounted for [*Liu et al.*, 1998]. Transports derived directly from ADCP sections in the upper 350 m taken at the same time as the geostrophic transports give a mean transport of 19.7 Sv. Using geostrophy to extend the ADCP velocity profiles to the sea bottom, the mean transport becomes 22.6 ± 3 Sv [*Liu et al.*, 1998], which is very close to our moored mean estimate of 21.5 Sv.

3.3. Annual Cycle

Seasonal cycles of Kuroshio transport in the ECS have not been well resolved using snapshots derived from hydrographic measurements. Estimates of the magnitude of the annual transport variation range from as little as 6 Sv to as much as 20 Sv and with considerable year-to-year variability [*Guan*, 1981; *Kawabe*, 1988; *Ichikawa and Beardsley*, 1993]. The uncertainty is likely due to the strong aliasing of shipboard survey data caused by the 100-day variability in Kuroshio transport. *Kawabe* [1988] found a strong seasonal variation in the sea level difference (SLD) across the Kuroshio at Tokara Strait with a maximum in summer and minimum in fall. *Johns et al.* [2001] showed that subtidal SLD time series across the ETC is significantly correlated with our 20-month moored transport record with a correlation coefficient of 0.70. Here we will use the Johns et al. regression relationship to derive transport from SLD across the ETC for our 20-month moored period and over a longer 7-year period that provides better resolution of the annual cycle.

Monthly averaged time series of moored transports are given in Figure 8a, together with transports derived from SLD across the ETC between Ishigaki Island and Keelung and Sverdrup transports derived from COADS winds over the Philippine Basin at 24.5°N, between 125°E and 142°E longitude. This zonal section was chosen to represent wind forcing over the Philippine Basin west of the Izu-Ogasawara and Mariana

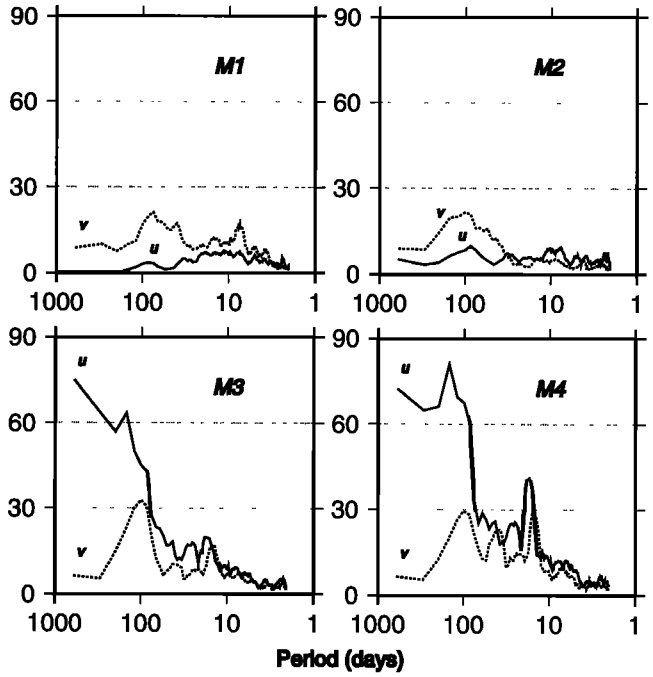

Figure 4. Variance conserving spectra of vertically averaged downstream (v) and cross-stream (u) currents from moorings M1–M4.

Ridges, which are sufficiently shallow to serve as a blocking mechanism of barotropic Rossby waves generated by wind forcing east of the ridge. The negative values of Sverdrup transports are plotted for better visual comparison with western boundary return transports in the ETC. There is generally good agreement between these monthly time series. The two fall minimum transports, two winter maximums, and single summer maximum are clearly evident in the measured and wind-driven transports. The most significant differences occurred during February 1995 when the Kuroshio transport was minimum due to strong interaction with a mesoscale eddy as discussed previously (and also discussed by *Zhang et al.* [2001]) and toward the end of the records.

Annual cycles of PCM-1 moored transports, sea level differences across the ETC and Sverdrup transports within the Philippine Sea are compared in Figure 8b. The moored transports show peaks during winter, spring, and summer. Maximum transport of ~27 Sv occurred in winter (December). The summer and spring maxima were ~25 Sv each. Transport minima were ~20 Sv in early spring and early summer and 19 Sv in fall. The annual transport pattern observed during this 20-month period is significantly correlated with the monthly averaged sea level difference across the ETC. The derived Sverdrup transports also show significant correlation with the moored transport cycle, although the peaks in Sverdrup transports tend to lead the observed transport peaks by ~1 month.

Because a significant 100-day variability was found in the Kuroshio transport time series (Figures 6 and 7) the observed annual cycle derived from our 20-month moored record could be significantly aliased. From transport measurements made previously off Abaco Bahamas, where there also occurred significant 100-day transport variations, we found that ~4 years of observations were required to clearly resolve the annual cycle [*Lee et al.*, 1996]. Longer records of sea level differences across the ETC are available, and our moored transports provide an excellent calibration for estimating longer-term volume transport records from these sea level difference time series. Therefore we use the regression relationship derived by *Johns et al.* [2001] to estimate volume transport from SLD time series over a 7-year period from April 1989 to May 1996 from tide gauges located at the Japanese island of Ishigaki, on the east side of the ETC, and at Keelung, on the northern tip of Taiwan (Figure 2).

The annual cycle computed for this 7-year time series is shown in Figure 9a together with each individual year of the 7-year SLD time series. The magnitude of the annual transport cycle computed over the 7-year period from SLD is ~4 Sv and consists of a maximum of 24 Sv in summer and a minimum of 20 Sv in fall. A weaker secondary maximum occurred in winter. During the PCM-1 time period the transport change from the summer maximum to fall minimum was 6 Sv from the moored currents and a similar change is also indicated by the SLD (Figure 8b). The maximum transport for the 7-year period occurred in July, which is in-phase with a summer peak in the Sverdrup transport within the Philippine Sea from Comprehensive Ocean-Atmosphere Data Set (COADS) winds (Figures 9 and 10b). Minimum transport occurred in October for both the longer and shorter record lengths and for the Sverdrup transports for both time periods. Seasonal cycles of SLD derived transports for each individual year of the 7-year period show considerable year-to-year variability, which accounts for the decreased magnitude of the range of the annual cycle when the individual records are averaged (Figure 9a). However, the summer maximum transport and fall minimum are robust features that repeat in 5 out of the 7 years, although not necessarily in the same month.

Monthly average transport time series from SLD for the complete 7-year period are shown in Figure 9b together with the negative of monthly average Sverdrup transports for the Philippine Basin. There is considerable agreement between these time series, but occasionally, there are also significant differences. The annual change of transport from SLD for the individual years ranges from ~4 to 10 Sv, whereas the predicted Sverdrup transport cycles range from ~15 to 30 Sv, with largest transports occurring in winter and minimum occurring in fall. This suggests that a significant annual transport cycle should occur east of the Ryukyu Island chain to help compensate for the wind forcing over the Philippine Sea. There is also a long-term trend of larger annual transport cycles occurring in both the SLD and Sverdrup time series during the first half of the 7-year record and decreasing over the second half of the record, during the PCM-1 moored measurements. The mean transport determined from the 7-year sea level difference record is 21.3 Sv, which compares well with our 21.5 estimate from the 20-month moored current data. The annual mean transport from the 7-year SLD time series ranged from a minimum of 19.9 Sv in 1994 to a maximum of 23 Sv in 1991, with an interannual variability of 1–2 Sv.

The annual transport cycle determined for the 7-year period is compared to available basin- and global-scale model results for the same time period (Figure 9c). The Naval Research Laboratory (NRL) 1/8° North Pacific model results were provided by H. Hurlburt and J. Metzger. This is a six-layer primitive equation model forced only by European Centre for Medium-Range Weather Forecasts (ECMWF) daily winds from 1981 to 1996, with the long-term mean replaced by the annual mean from *Hellerman and Rosenstein* [1983]. We also compare

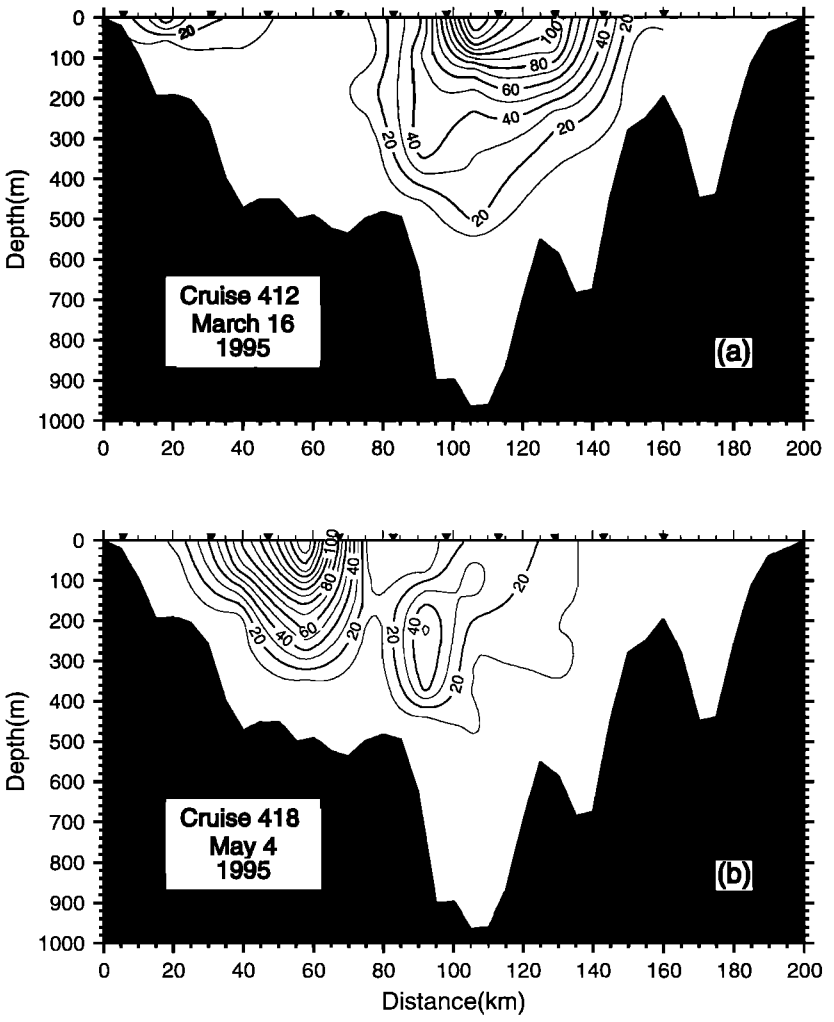

Figure 5. Kuroshio geostrophic velocity structure across the PCM-1 moored array from hydrographic cruises of Taiwan R/V *Ocean Researcher I* on March 16 and May 4, 1995. Triangles show station locations (from Figure 3 of *Johns et al.* [1995]).

results from two versions of the Semtner-Chervin global model: the 1/4° Parallel Ocean Climate Model (POCM) provided by R. Tokmakian of the Naval Postgraduate School, and the 1/6° Parallel Ocean Program (POP) model provided by R. Malone of Los Alamos National Laboratory. The POCM simulation was run for a 3-year period, 1994–1996. These models are forced with 3-day average ECMWF wind stress and a surface heat flux climatology. All three models have been compared with satellite altimetry and appear to reasonably represent the mesoscale variations in the Kuroshio extension region

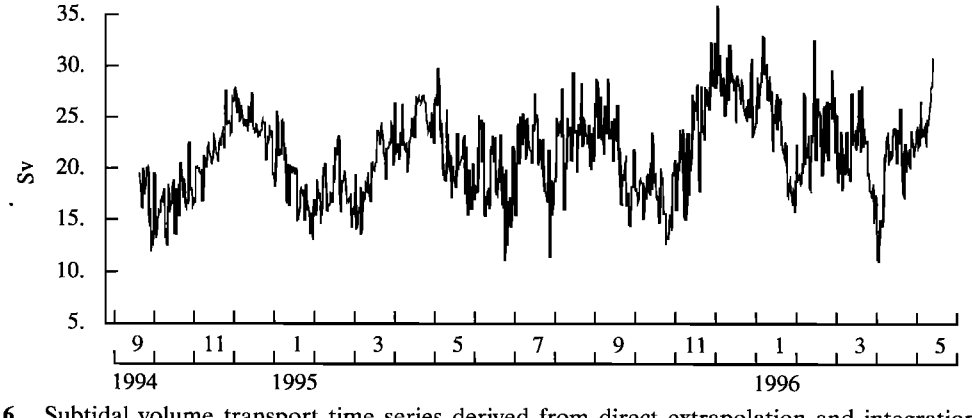

Figure 6. Subtidal volume transport time series derived from direct extrapolation and integration of the downstream current field from the PCM-1 moored array.

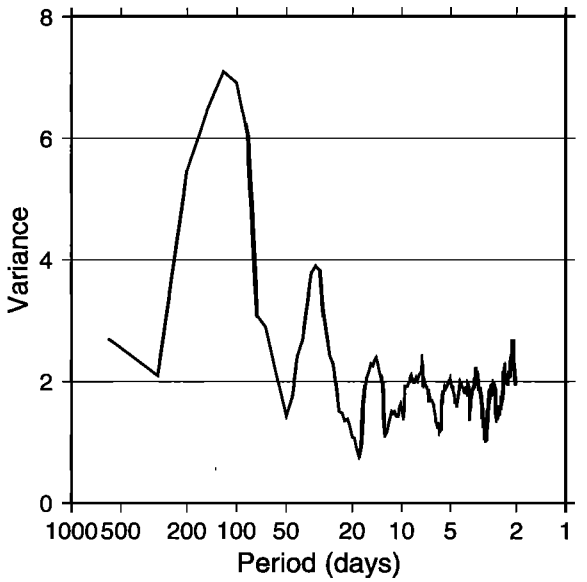

Figure 7. Variance conserving spectra of PCM-1 moored transport time series.

[*Hurlburt et al.*, 1996; *Mitchell et al.*, 1996; *Stammer et al.*, 1996; *McClean et al.*, 1997].

Over the 7-year time period both the NRL and POP models show annual transport cycles of the Kuroshio in the ETC that generally agree with that of the SLD time series (Figures 9c and 9a). The magnitudes of the annual transport cycles from the models are similar to that observed, except the NRL model has a stronger fall minimum transport and greater winter maximum, and the summer maximum is spread out over the summer and spring period. The annual cycle of the POP model is slightly weaker than observed, and the POCM cycle has a weak fall minimum, as well as a winter minimum that is not observed.

4. Discussion: Comparison of the Kuroshio at 24.5°N With the Florida Current

Comparisons between the Kuroshio and Gulf Stream systems have been made by many authors dating to the study of *Worthington and Kawai* [1972]. The Kuroshio in the East China Sea is analogous to the Florida Current where it is trapped in the Straits of Florida between the Florida peninsula and the Bahamas. The Florida Current has been intensively studied with moored current meter observations and other techniques for many years, with the most recent and comprehensive study being the Subtropical Atlantic Climate Studies (STACS) program [*Molinari et al.*, 1985; *Leaman et al.*, 1987; *Schott et al.*, 1988; *Larsen*, 1992]. The PCM-1 measurement program was modeled in many ways after the STACS program and provides a unique opportunity to compare the detailed behavior of these two current systems. Here we compare three specific aspects of Kuroshio and Florida Current systems: (1) their seasonal cycles, (2) their mesoscale variability, and (3) their mean transport and contributions to gyre closure in their respective basins.

4.1. Seasonal Cycles

In contrast to the Kuroshio the annual cycle of Florida Current transport (Figure 10a) has been well-established with a maximum of ~33 Sv in July and August and a minimum in

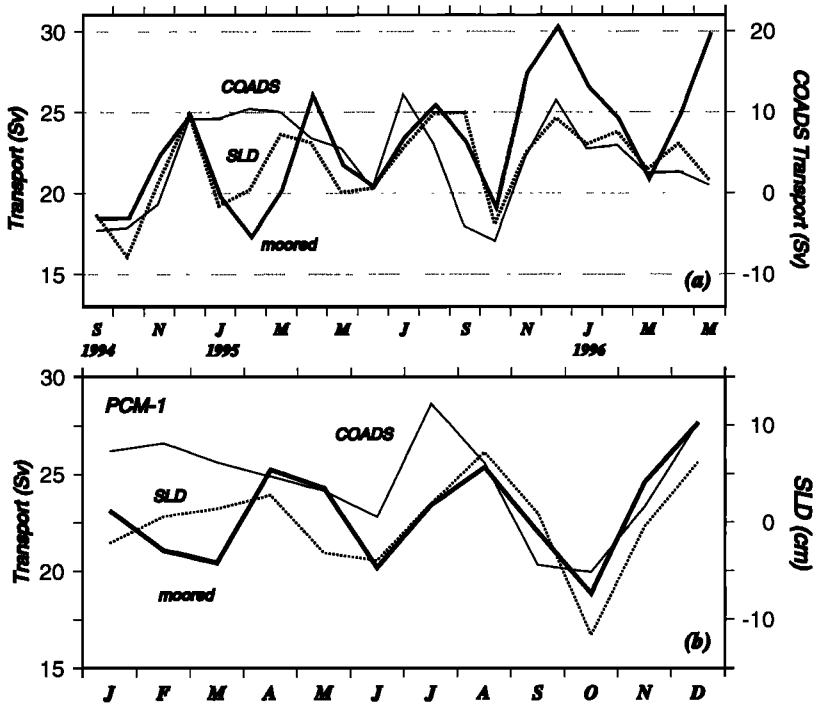

Figure 8. (a) Monthly average transports over the 20-month PCM-1 record for moored transports (moored), transports derived from sea level differences (SLD), and negative values of Sverdrup transports between 125° and 142°E longitude (Comprehensive Ocean-Atmosphere Data Set (COADS)). (b) Annual cycles derived from monthly averages of moored and interior Sverdrup transports (left scale) and SLD (right scale) for the 20-month moored record period.

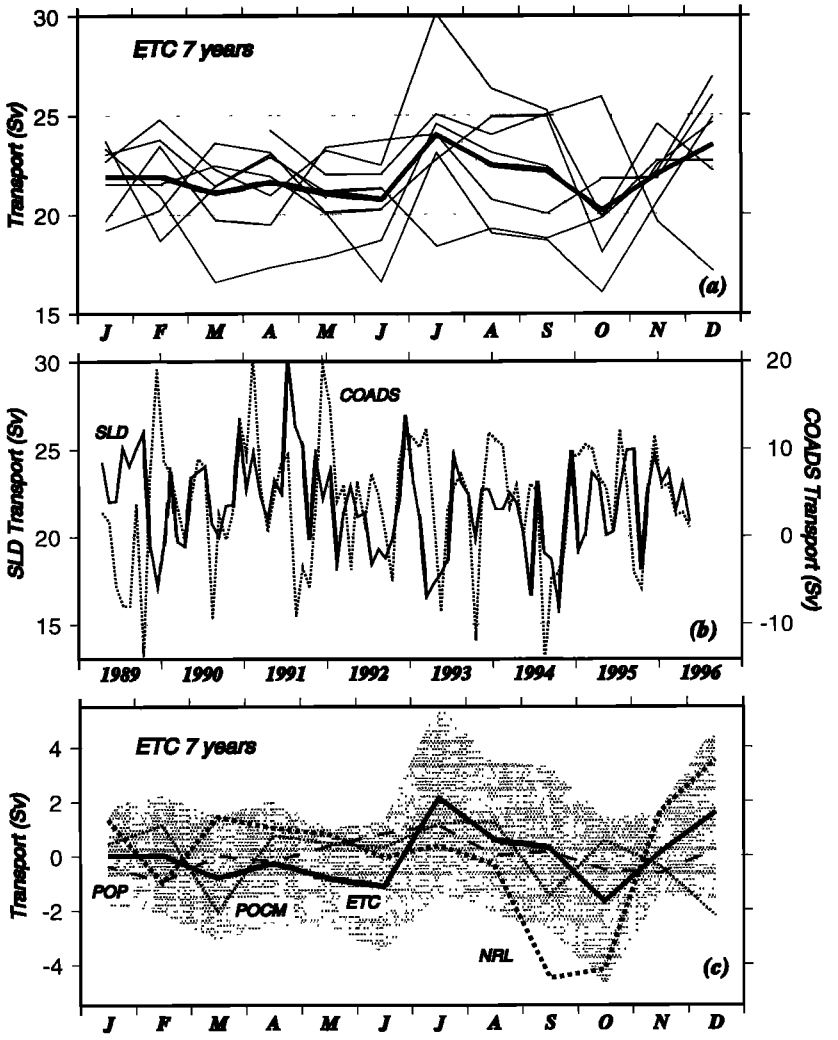

Figure 9. (a) Annual transport cycles derived from a 7-year SLD record between Ishigaki Island and Keelung (bold) and for each individual year during the period April 1989 to May 1996. (b) Monthly average transports from SLD and COADS for the 7-year period April 1989 to May 1996. (c) Annual transport cycle from SLD and results from Naval Research Laboratory (NRL) and Parallel Ocean Program (POP) models for 7-year period April 1989 to May 1996 and Parallel Ocean Climate Model (POCM) for 3 years, 1994–1996. The shaded area represents the envelope of total transport variability from Figure 9a.

October and November of ~26 Sv [*Niiler and Richardson*, 1973; *Molinari et al.*, 1985; *Schott and Zantopp*, 1985; *Leaman et al.*, 1987; *Schott et al.*, 1988; *Rosenfeld et al.*, 1989]. The annual cycle has been attributed to the combined influence of local along-channel wind forcing [*Lee and Williams*, 1988; *Schott et al.*, 1988], remote wind forcing from the wind stress curl in the Caribbean [*Schott and Zantopp*, 1985], and topographic Kelvin waves from wind forcing over the variable topography of the northwest Atlantic [*Anderson and Corry*, 1985]. Numerical simulations by *Anderson and Corry* [1985] clearly showed that the annual cycle of Sverdrup transport, which is maximum in winter and minimum in fall (Figure 10a), is effectively blocked by the shallow topography of the Bahamas from influencing the flow in the Straits of Florida; that is, the barotropic Rossby waves are blocked and compensation by baroclinic Rossby waves will take of the order of a decade. However, their model shows a robust wind forced annual transport cycle of ±13 Sv in boundary currents seaward of the Bahamas that was recently substantiated with moored observations [*Lee et al.*, 1996], with remarkable agreement in magnitude and phase of the annual cycles of Sverdrup transports computed west of the Mid-Atlantic Ridge and the moored values.

A 19-year sea level difference time series measured across the Tokara Strait shows a pronounced annual cycle similar to that of the Florida Current [*Kawabe*, 1988]. Here we compare seasonal cycles of sea level difference across the Tokara Strait from Kawabe's time series to our 7-year records across the ETC (Figure 10b). Also shown are the negative Sverdrup transports between 125°E and 142°E for the same 7-year period (Figure 10b). Clearly, the summer maximum and fall minimum of SLD occur with similar magnitude at the Kuroshio's entrance and exit to the East China Sea despite the different record lengths and measurement periods of the sea level differences. The primary distinction between the two data sets are a more sharply defined summer maximum in the ETC, as well as a second winter maximum at this location. The annual cycle of Sverdrup transports in the Philippine Sea is almost identical

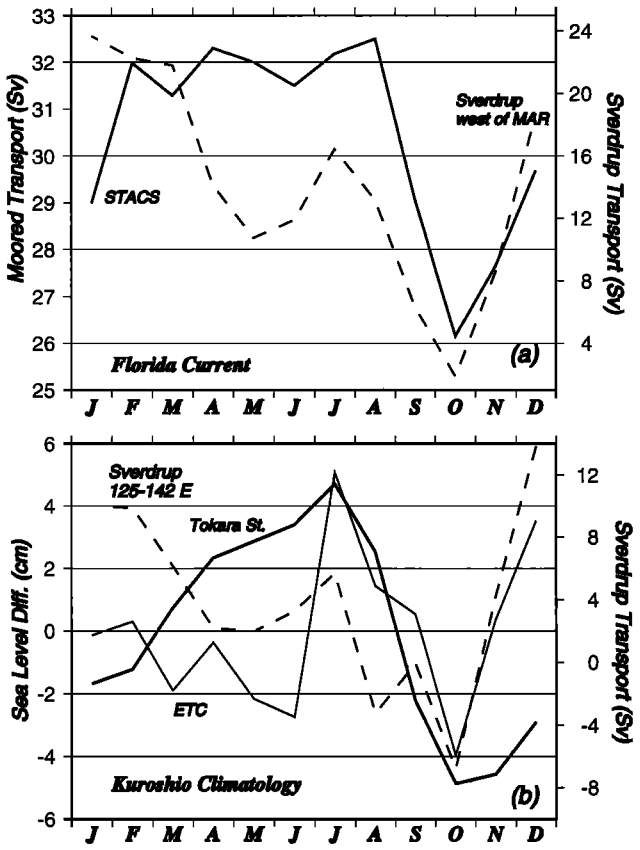

Figure 10. (a) Annual cycle of Florida Current transport [from *Schott et al.*, 1988] and negative Sverdrup transports at 27°N between the Bahamas and the Mid-Atlantic Ridge in the Atlantic. (b) Annual cycles of SLD across the Tokara Strait from *Kawabe*'s [1988] 19-year record plotted with SLD across the ETC from the 7-year record (April 1989 to May 1996) and negative Sverdrup transports between 125°E and 142°E longitude from COADS winds during the same 7-year period.

to that found for 27°N in the Atlantic west of the Mid-Atlantic Ridge and consists of a winter maximum and fall minimum and a secondary semiannual transport peak in the summer (Figures 10a and 10b). This pattern is similar to the seasonal SLD cycle in the ETC, indicating that the seasonal SLD and Kuroshio transport cycles are necessary in part to compensate for wind forcing over the Philippine Basin. The good agreement between the annual transport cycle derived from the 7-year SLD record for the ETC with that determined from wind-forced models on basin and global scales (Figure 9c) provides further support to the importance of wind forcing on the Kuroshio annual transport cycle at this location. The annual range of Sverdrup transports in the Philippine Sea between the winter maximum and fall minimum was ~20 Sv, whereas in the ETC during this same time period the annual range estimated from SLD time series was 4 Sv. This suggests that an annual transport cycle should occur east of the Ryukyu Islands with a mean range of ~16 Sv to balance the annual cycle of wind forcing west of the Izu-Ogasawara and Mariana Ridges. The lack of a winter maximum in SLD across the Tokara Strait indicates that the annual Sverdrup transport cycle in the Philippine Sea is blocked from entering the ECS by the Ryukyu Island chain. A similar conclusion was arrived at by *Sekine and Kutsuwada* [1994] from a numerical model study of transport responses to seasonal wind forcing over the western Pacific. They also found a winter transport maximum seaward of the Ryukyu Island chain.

There is a remarkable similarity of the annual Florida Current and Kuroshio transport cycles and between the seasonal variations of Sverdrup transports west of the midbasin ridges in both oceans. The annual transport cycle in both currents is maximum in summer and minimum in fall with amplitudes of ±3 Sv for the Florida Current (Figure 10a) and ±2 Sv for the Kuroshio (Figures 9a and 10b). The annual Sverdrup transport cycle in both regions is maximum in winter and minimum in fall with amplitudes of ±11 Sv in the western Atlantic and ±10 Sv in the western Pacific (Figures 10a and 10b). There are also secondary summer maxima in Sverdrup transport in both oceans. The lack of a winter transport maximum in the Florida Current and Kuroshio inside the ECS at the Tokara Strait appears to result from the topographic blocking of barotropic Rossby waves by the Antilles and Ryukyu Island chains, respectively. However, the Kuroshio in the ETC also displays a secondary winter maximum due to its open connection to the Philippine Sea to the south. This mismatch in the strength of the winter maximum Sverdrup forcing in the northwest Pacific compared to the size of the winter peak in Kuroshio transport is similar to that found in the Atlantic (Figures 10a, 10b, and 9a) and indicates that a large annual transport cycle of ±8 Sv may occur east of the Ryukyus, similar to the ±13 Sv annual transport cycle predicted and observed east of the Bahamas [*Anderson and Corry*, 1985; *Lee et al.*, 1996].

To investigate the cause of the annual cycle of sea level differences in the Tokara Strait, we ran a correlation between the sea level differences and the *Hellerman and Rosenstein* [1983] seasonal wind stress components from the equator to 45°N in the Pacific. Correlations of 0.9 and higher are found along the northwest boundary of the Pacific between the meridional component of the wind stress and sea level difference, with the wind stress leading by 1 month (Figure 11). This indicates that the annual cycle of Kuroshio transport in the East China Sea may have additional contribution from local along-channel wind forcing, similar to that found for the Atlantic [*Lee and Williams*, 1988; *Schott et al.*, 1988]. *Ichikawa and Beardsley* [1993] also found evidence for local along-channel wind forcing of Kuroshio transport in the ECS. As in the Atlantic, the local contribution would come from increased northward wind component over the eastern ECS in the summer and increased southward winds over this region in fall. *Lee and Williams* [1988] showed that in the Straits of Florida a barotropic transport response to local synoptic-scale along-channel wind forcing could explain a significant fraction of the winter subtidal transport variability, as well as the annual transport cycle of the Florida Current. The physical mechanism involved in the process is similar to the barotropic shelf response to along-shelf wind forcing.

4.2. Mesoscale Variability

The transport spectra of the Kuroshio and Florida Current systems are compared in Figure 12, which shows that there are considerable differences in the variability characteristics of the two current systems. While the spectral energy levels are similar for periods shorter than ~20 days and again near the annual timescale, the 100-day peak that dominates the Kuroshio transport spectrum is absent in the Florida Current. The Florida Current, in fact, has a flat or even slightly depressed energy level at these several month timescales compared to the

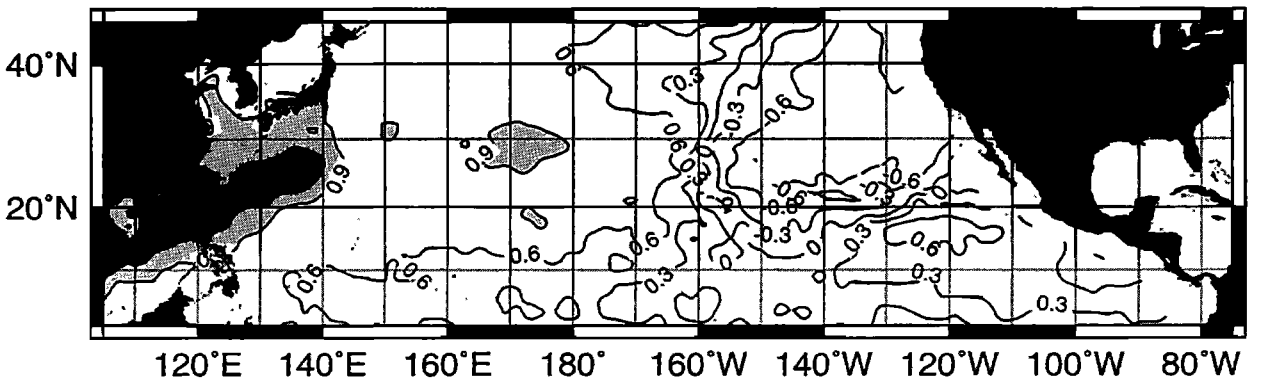

Figure 11. Correlation map of monthly averaged sea level differences across the Tokara Strait from *Kawabe*'s [1988] 19-year record with *Hellerman and Rosenstein*'s [1983] seasonal meridional wind stress.

synoptic (days to weeks) and seasonal bands. As a result, the overall transport variability of the Kuroshio is considerably larger than that of the Florida Current. The transport variance of the Kuroshio derived from the PCM-1 array is ~20 Sv^2 (based on the standard deviations of 4.1–4.8 Sv obtained from the different derivation methods of *Johns et al.* [2001]) versus ~10 Sv^2 for the Florida Current (standard deviation of 3.0–3.5 Sv [*Leaman et al.*, 1987; *Schott et al.*, 1988]). Thus, in terms of variance the transport variability of the Kuroshio is nearly twice as large as that of the Florida Current. Perhaps surprisingly, the total range of transport variations of the two currents is not substantially different. The Florida Current transport ranges between ~20 and 40 Sv [*Schott et al.*, 1998; *Larsen*, 1992], roughly the same range as the 11–36 Sv variations of the Kuroshio in the ETC (Figure 6). However, the Florida Current variations of this magnitude tend to be restricted to timescales of several days to weeks instead of the several month timescales seen in the PCM-1 array data. The Kuroshio also can exhibit large transport variations on timescales of days to weeks, similar in magnitude to those in the Florida Current but with considerably less variance than the 100-day periods.

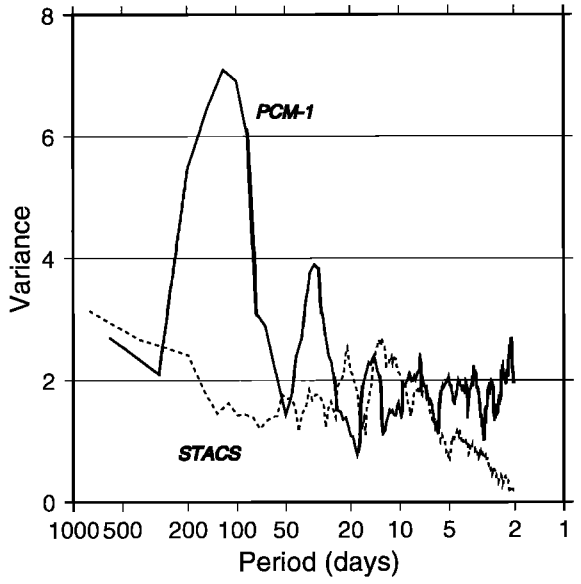

Figure 12. Variance conserving spectra of transport variations in the Kuroshio at 24°N in the ETC (PCM-1) and the Florida Current at 27°N in the Straits of Florida (STACS).

The reason for this large difference in spectral characteristics appears to be the relative isolation of the Florida Current from the ocean interior as compared to the Kuroshio where it enters the ECS. The ETC is open to the Philippine Basin to the south and therefore may be strongly influenced by ocean mesoscale features that propagate into the western boundary region from the ocean interior. Conversely, the Florida Current is topographically isolated from the ocean interior by the Antilles Island chain and the Bahamas. As shown by *Zhang et al.* [2001], the 100-day period fluctuations in the Kuroshio transport at the PCM-1 section are closely linked to mesoscale eddy features with this same periodicity that propagate westward from the interior along the latitude of the subtropical convergence. These eddies cause large meanders of the Kuroshio to form along the southeast coast of Taiwan which strongly perturb the Kuroshio transport entering the ETC. Such eddy features are also present off the Bahamas in the western subtropical Atlantic [*Lee et al.*, 1990, 1996; *Halliwell et al.*, 1991], but they are apparently blocked from penetrating into the Straits of Florida by the Antilles and Bahamas island chains. While the Ryukyu Islands may play a role similar to the Bahamas in blocking part of the interior ocean eddy signal from directly influencing the ECS from the east, there is no counterpart to the Antilles Island chain and Caribbean Sea in the Pacific to block it from direct ocean influences to the south. Thus the Kuroshio at the ECS may experience large fluctuations on the open ocean mesoscale (several month) timescale, whereas the Florida Current is effectively isolated from these influences.

4.1.3. Mean transports and gyre closure. Western boundary currents of subtropical gyres provide the closure for the interior circulation resulting from net wind and thermohaline forcing. Comparison of mean transports in the western boundary regions of the North Atlantic and North Pacific subtropical gyres are shown in Figure 13. The mean transport of the Florida Current at 27°N is ~31.5 Sv [*Leama et al.*, 1987], which is ~10 Sv larger than the Kuroshio transport at the PCM-1 section. The smaller Kuroshio transport occurs despite a larger wind-driven Sverdrup transport in the North Pacific subtropical gyre at this latitude than in the Atlantic. We estimate the mean southward Sverdrup transport across 24°N in the Pacific from COADS winds to be ~33 Sv, while in the Atlantic it is ~26 Sv [*Leetma et al.*, 1977; *Schmitz et al.*, 1992;

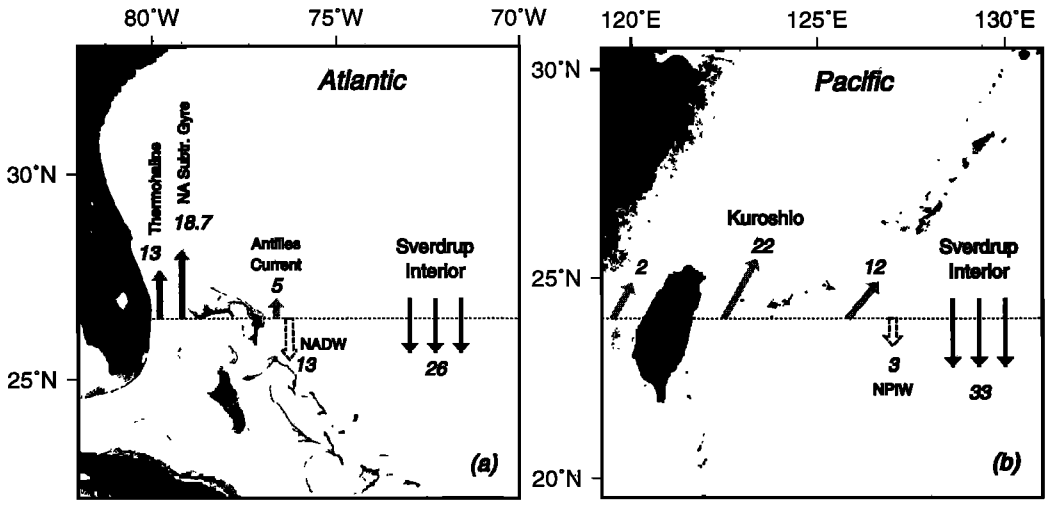

Figure 13. Mean transports (Sv) in the western boundary regions of the (a) North Atlantic and (b) North Pacific subtropical gyres needed to balance interior Sverdrup and thermohaline circulations. Net thermohaline interior transports are shown with dashed arrows, Sverdrup interior transports with solid arrows, and western boundary return transports with shaded arrows.

Lee et al., 1996]. *Hautala et al.* [1994] made a similar estimate and found the basin-scale geostrophic transport to be in approximate Sverdrup balance with wind-driven geostrophic transports. In addition to differences in the wind-driven Sverdrup transport in the two basins, the different thermohaline circulations need to be taken into account in assessing the strength of the two boundary currents. The meridional overturning cell in the Atlantic contributes ~13 Sv to the transport of the Florida Current to balance the export of North Atlantic Deep Water (NADW) from the basin [*Schmitz and Richardson*, 1991]. However, in the North Pacific, only ~3 Sv of the western boundary return flow may be attributed to a thermohaline component which takes part in the formation of North Pacific Intermediate Water (NPIW) off northeast Japan and its subsequent spread around the subtropical gyre [*Talley*, 1993]. The Florida Current transport of 31.5 Sv thus carries ~80% of the combined northward wind-driven gyre and thermohaline return flows in the Atlantic (~39 Sv), while the Kuroshio transport of 21.5 Sv in the ETC appears to account for only ~60% of the combined flows in the Pacific (~36 Sv). Model results and hydrographic data indicate that ~1–3 Sv northward mean flow may occur in the Taiwan Strait between Taiwan and mainland China [*Guan*, 1994; *Fang and Zhao*, 1988]. This would reduce the northward flow east of the Ryukyus, required for gyre closure, to ~12 Sv.

In both Atlantic and Pacific cases a significant northward western boundary flow occurs seaward of offshore island chains that tend to separate a portion of the flow, the Bahamas and Ryukyu Islands, respectively. In the Atlantic, ~7 Sv are required to balance the net gyre and thermohaline circulation budgets [*Schmitz et al.*, 1992]. Recently, *Lee et al.* [1996] have substantiated the existence of this Antilles Current from direct moored measurements, showing a mean northward flow of ~5 Sv that is entirely wind forced and accounts for 20–25% of the Sverdrup return flow. However, in the Pacific a northward mean flow of 12 Sv is called for east of the Ryukyus to balance the subtropical gyre circulation. The mean flow east of the Ryukyus amounts to ~36% of the interior Sverdrup circulation, which leaves ~58% of the Sverdrup circulation to be carried by the Kuroshio, provided we assume that the Kuroshio also carries all of the interior thermohaline circulation, as takes place in the Gulf Stream [*Schmitz et al.*, 1992; *Lee et al.*, 1996].

Our estimates of mean boundary current flows in the Pacific compare well with values from other sources. *Ichikawa and Beardsley* [1993] reported a 3-year average Kuroshio transport in the East China Sea of 23.7 Sv from combined hydrographic and surface current data. They estimated a northward barotrophic flow east of the Ryukyu Islands of 11.4 Sv. Also *Yuan et al.* [1994, 1998], estimated a northward flow of 10–15 Sv east of the Ryukyus using an inverse method with hydrographic and current meter measurements. Similarly, the POP model results predict a mean Kuroshio flow of 23 Sv in the ETC and 11 Sv northward flow for the boundary region east of the Ryukyus.

5. Summary and Conclusions

A 20-month time series of Kuroshio volume transport was derived from a moored current meter array deployed across the East Taiwan Channel at 24.5°N from September 19, 1994, to May 27, 1996. Transport variations ranged from a maximum of 36 to a minimum of 11 Sv with a standard deviation of ±4.8 Sv. Significant transport variability occurred on 100-day and seasonal timescales. Less energetic transport fluctuations occurred at periods of 10–15 and 30–40 days. Mean current structure consisted of a surface intensified downstream jet with maximum estimated currents of 100 cm/s located on the western side of the channel ~50 km from the Taiwan coast. Strong 100-day current and transport events were found to be associated with meandering of the current axis from the west to the east side of the channel. When the axis is located on the east side of the channel, the downstream flow appears to split with part flowing to the east along the southern flank of the Ryukyu Island chain and part curving to the west, causing strong westward flow and decreased temperature through the channel and a minimum in downstream transport. The cause of these 100-day meander and transport events are shown by *Zhang et al.*

[2001] to be associated with the arrival of warm mesoscale eddies from the interior. Interestingly, a similar process was recently observed near the same latitude in the Atlantic off Abaco Bahamas, where warm mesoscale eddies from the interior were found to merge with the western boundary currents and to cause large transport variations and meandering with a similar 100-day period [*Lee et al.*, 1996].

Monthly averages of moored transports were found to be significantly correlated with sea level differences across the ETC and with Sverdrup transports computed from the zonal integration of the wind stress curl over the Philippine Sea between 125°E and 142°E longitude. This longitude band is west of the Izu-Ogasawara and Mariana Ridges, which are sufficiently shallow as to block barotropic Rossby waves from transmitting wind-driven transport signals from the ocean interior.

A 7-year transport time series derived from these sea level differences across the ETC produced a annual transport cycle with a maximum of 24 Sv in the summer and minimum of 20 Sv in the fall. Although considerable interannual variability of the amplitude of the annual cycle occurred during this period, maximum transports were consistently found in summer and minimum transports in fall. There was also a secondary maximum in winter. The annual range of Sverdrup transports during this seven year period was 20 Sv, which indicates that a significant western boundary current with a seasonal variation of ±8 Sv is needed east of the Ryukyus to balance the wind forcing over the Philippine Sea. Kuroshio annual transport cycles at the ETC were also found to be in general agreement in amplitude and phase with available results from basin-scale wind-forced models for the 7-year period.

The annual transport cycle of the Kuroshio is remarkably similar to that of the Florida Current in both amplitude and phase and may also result from a combined response to local and remote wind forcing, as was found for the Florida Current [*Lee and Williams*, 1988; *Schott et al.*, 1988]. Seasonal changes in local along-channel winds over the ECS are highly correlated with SLD time series from the Tokara Strait that is a measure of transport. In addition, *Ichikawa and Beardsley* [1993] found a positive correlation between downstream wind stress and transport in the ECS that did not occur outside of the ECS. However, the ETC is open to the south so is not isolated from interior wind forcing responses as occurs in the Straits of Florida due to the Bahamas and Antilles Island chains. As a result, the seasonal cycle of Kuroshio transport in the ETC matches reasonably well with the seasonal cycle of the Sverdrup wind forced transports over the Philippine Sea and with wind-forced models, showing both a summer and winter maximum and a fall minimum. In the Straits of Florida the remotely forced portion of the annual transport cycle was due to wind-forced Kelvin wave generation northeast of the straits [*Anderson and Corry*, 1985].

Our moored estimate of the annual mean Kuroshio volume transport in the ETC is 21.5 ± 2.5 Sv. This flow is required as partial balance of the mean Sverdrup transport across the interior of the Pacific at this latitude of 33 Sv plus 3 Sv thermohaline flow to compensate for the formation of North Pacific Intermediate Water [*Talley*, 1993]. Observations and model results also indicate that a mean northward flow of ~2 Sv occurs west of Taiwan. Thus a mean northward flow of ~12 Sv is needed east of the Ryukyu Islands to complete the balance of wind and thermohaline forced flows at this latitude. These estimates of mean flows for the Kuroshio and the eastern boundary of the Ryukyus are in excellent agreement with those made earlier by *Ichikawa and Beardsley* [1993] of 23.7 and 11.4 Sv, respectively, with POP model results of 23 and 11 Sv, and with shipboard estimates in the ETC of 22.6 Sv [*Liu et al.*, 1998]. To date, there have been no direct moored measurements of transports east of the Ryukyus.

Acknowledgments. Funding for this project was provided by the National Science Foundation (NSF grant OCE9302187) for the U.S. participation. The Taiwan WOCE Program was supported by the National Science Council. We greatly appreciate the assistance rendered by the personnel of R/V *Ocean Researchers* I and II in deployment and recovery of moorings. We thank Harley Hurlburt and Joe Metzger of the Navy Research Lab, R. Tokmakian of the Naval Post Graduate School, and R. Malone of Los Alamos National Lab for providing modeling results for comparison with our observations. We are thankful for the kind assistance of Hiroshi Yoshioka for helping us to obtain sea level and wind data from the Japanese Meteorological Agency. Special appreciation is extended to the RSMAS Marine Technology Group, Phil Bedard, Mark Graham, and Robert Jones for their dedication to mooring preparation and shipboard deployments. Final word processing of this manuscript was aided by the help of Elizabeth Maldonado.

References

Akima, H., A new method of interpolation and smooth curve fitting based on local procedures, *J. Assoc. Comput. Mach.*, *17*, 589–602, 1970.

Anderson, D. L., and R. A. Corry, Seasonal transport variations in the Florida Straits: A model study, *J. Phys. Oceanogr.*, *15*, 773–786, 1985.

Bingham, F. M., and L. D. Talley, Estimates of Kuroshio transport using an inverse technique, *Deep Sea Res.*, *38*, 521–545, 1991.

Bryden, H. L., D. H. Roemmich, and J. A. Church, Ocean heat transport across 24°N in the Pacific, *Deep Sea Res.*, *38*, 297–324, 1991.

Fang, G., and B. Zhao, A note on the main forcing of the northeastward flowing current off the southeast China coast, *Prog. Oceanogr.*, *21*, 373–372, 1988.

Fujiwara, I., Y. Hanzawa, I. Eguchi, and K. Hirano, Seasonal oceanic conditions on a fixed line in the East China Sea, *Oceanogr. Mag.*, *37*, 37–46, 1987.

Guan, B., Analysis of the variations of volume transports of the Kuroshio in the east China Sea, paper presented at Japan-China Symposium on Physical Oceanography and Marine Engineering in the East China Sea, Inst. of Oceanic Res., Tokai Univ., Tokyo, 1981.

Guan, B., Patterns and structures of the currents in Bohai, Huanghai and East China Seas, in *Oceanology of China Seas*, vol. 1, edited by D. Zhou, Y.-B. Liang, and C.-K. Zeng, pp. 17–26, Kluwer Acad., Norwell, Mass., 1994.

Halliwell, G. R., Jr., P. Cornillon, and D. A. Byrne, Westward propagating SST anomaly features in the Sargasso Sea, 1982–1988, *J. Phys. Oceanogr.*, *21*, 635–649, 1991.

Hasunuma, K., and K. Yoshida, Splitting of the subtropical gyre in the western North Pacific. *J. Oceanogr. Soc. Jpn.*, *34*, 160–172, 1978.

Hautala, S. L., D. H. Roemmich, and W. J. Schmitz Jr., Is the North Pacific in Sverdrup balance along 24°N?, *J. Geophys. Res.*, *99*, 16,041–16,052, 1994.

Hellerman, S., and M. Rosenstein, Normal monthly wind stress over the world ocean with error estimates, *J. Phys. Oceanogr.*, *13*, 1093–1104, 1983.

Hurlburt, H. E., A. J. Wallcraft, W. J. Schmitz Jr., P. J. Hogan, and E. J. Metzger, Dynamics of the Kuroshio/Oyashio current system using eddy-resolving models of the North Pacific Ocean, *J. Geophys. Res.*, *101*, 941–976, 1996.

Ichikawa, H., and R. C. Beardsley, Temporal and spatial variability of volume transport of the Kuroshio in the East China Sea, *Deep Sea Res., Part I*, *40*, 583–605, 1993.

Imawaki, S., H. Uchida, H. Ichikawa, M. Fukasawa, S. Umatani, and the ASUKA Group, Satellite altimeter monitoring the Kuroshio transport south of Japan, *Geophys. Res. Lett.*, *28*, 17–20, 2001.

Johns, W. E., T. N. Lee, C.-T. Liu, and D. Zhang, PCM-1 array monitors Kuroshio transport, *WOCE Notes*, *7*, 10–13, 1995.

Johns, W. E., T. N. Lee, D. Zhang, R. Zantopp, C. T. Liu, and Y. Yang, The Kuroshio east of Taiwan: Moored transport observations

from the WOCE PCM-1 array, *J. Phys. Oceanogr.*, *31*, 1031–1053, 2001.

Kawabe, M., Variability of Kuroshio velocity assessed from the sea-level difference between Naze and Nishinoomote, *J. Oceanog. Soc. Jpn.*, *44*, 293–304, 1988.

Larsen, J. C., Transport and heat flux of the Florida Current at 27°N derived from the cross-stream voltages and profiling data: Theory and observations, *Philos. Trans. R. Soc. London*, *338*, 169–236, 1992.

Leaman, K., R. Molinari, and P. Vertes, Structure and variability of the Florida Current at 27°N: April 1982–July 1984, *J. Phys. Oceanogr.*, *17*, 565–583, 1987.

Lee, T. N., and E. J. Williams, Wind forced transport fluctuations of the Florida Current, *J. Phys. Oceanogr.*, *18*, 937–946, 1988.

Lee, T. N., F. Schott, and R. Zantopp, Florida Current: Low-frequency variability of the Florida Current as observed with moored current meter stations during April 1982–June 1983, *Science*, *227*, 298–301, 1985.

Lee, T. N., W. E. Johns, F. Schott, and R. Zantopp, Western boundary current structure and variability east of Abaco, Bahamas at 26.5°N, *J. Phys. Oceanogr.*, *20*, 446–466, 1990.

Lee, T. N., W. E. Johns, R. Zantopp, and E. Fillenbaum, Moored observations of western boundary current variability and thermohaline circulation at 26.5°N in the subtropical North Atlantic, *J. Phys. Oceanogr.*, *26*, 962–983, 1996.

Leetma, A., P. P. Niiler, and H. Stommel, Does the Sverdrup relation account for the Mid-Atlantic circulation?, *J. Mar. Res.*, *35*, 1–10, 1977.

Liu, C.-T., S.-P. Cheng, W.-S. Chuang, Y. Yang, T. N. Lee, W. E. Johns, and H.-W. Li, Mean structure and transport of Taiwan Current (Kuroshio), *Acta Oceanogr. Taiwan.*, *36*, 159–176, 1998.

McClean, J. L., A. J. Semtner, and V. Zlotnicki, Comparisons of mesoscale variability in the Semtner-Chervin 1/4° model, the Los Alamos Parallel Ocean Program 1/6° model, and TOPEX/Poseidon data, *J. Geophys. Res.*, *102*, 25,203–25,226, 1997.

Mitchell, J. L., W. J. Teague, G. A. Jacobs, and H. E. Hurlburt, Comparisons of eddy-resolving model simulations and GEOSAT-ERM altimetry in the Kuroshio extension, *J. Geophys. Res.*, *101*, 1045–1058, 1996.

Molinari, R. L., W. D. Wilson, and K. Leaman, Volume and heat transports of the Florida Current: April 1982 through August 1983, *Science*, *227*, 295–297, 1985.

Niiler, P. P., and W. S. Richardson, Seasonal variability of the Florida Current, *J. Mar. Res.*, *31*, 144–167, 1973.

Nitani, H., Beginning of the Kuroshio, in *The Kuroshio*, edited by H. Stommel and K. Yoshida, pp. 129–163, Univ. of Wash. Press, Seattle, 1972.

Olson, D. B., F. Schott, R. Zantopp, and K. Leaman, The mean circulation east of the Bahamas as determined from historical XBT data and a recent measurement program, *J. Phys. Oceanogr.*, *14*, 1470–1487, 1984.

Qiu, B., and R. Lukas, Seasonal and interannual variability of the north Equatorial Current, the Mindanao Current, and the Kuroshio along the Pacific western boundary, *J. Geophys. Res.*, *101*, 12,315–12,330, 1996.

Roemmich, D., and T. McCallister, Large scale circulation of the North Pacific Ocean, *Prog. Oceanogr.*, *22*, 171–204, 1989.

Rosenfeld, L. K., R. L. Molinari, and K. D. Leaman, Observed and modeled annual cycle of transport in the Straits of Florida and east of Abaco Island, the Bahamas (26.5°N), *J. Geophys. Res.*, *94*, 4867–4878, 1989.

Schmitz, W. J., and W. S. Richardson, On the transport of the Florida Current, *Deep Sea Res.*, *15*, 679–693, 1968.

Schmitz, W. J., and P. L. Richardson, On the sources of the Florida Current, *Deep Sea Res.*, *38*, suppl. 1, S379–S409, 1991.

Schmitz, W. J., J. D. Thompson, and J. R. Luyten, The Sverdrup circulation for the Atlantic along 24°N, *J. Geophys. Res.*, *97*, 7251–7256, 1992.

Schott, F., and R. Zantopp, Florida Current: Seasonal and interannual variability, *Science*, *227*, 308–311, 1985.

Schott, F., T. N. Lee, and R. Zantopp, Variability of structure and transport of the Florida Current in the period range of days to seasonal, *J. Phys. Oceanogr.*, *18*, 1209–1230, 1988.

Sekine, Y., and K. Kutsuwada, Seasonal variation in volume transport of the Kuroshio south of Japan, *J. Phys. Oceanogr.*, *24*, 261–272, 1994.

Stammer, D., R. Tokmakian, A. J. Semtner, and C. Wunsch, How well does a 1/4° global circulation model simulate large-scale oceanic observations? *J. Geophys. Res.*, *101*, 25,779–25,811, 1996.

Talley, L. D., Distribution and formation of North Pacific Intermediate Water, *J. Phys. Oceanogr.*, *23*, 517–537, 1993.

White, W., and K. Hasunuma, Interannual variability in the baroclinic gyre, *J. Mar. Res.*, *38*, 651–672, 1980.

Worthington, L. V., and H. Kawai, Comparison between deep sections across the Kuroshio and the Florida Current and Gulf Stream, in *Kuroshio: Physical Aspects of the Japan Current*, edited by H. Stommel and K. Yoshida, pp. 371–385, Univ. of Wash. Press, Seattle, 1972.

Yang, Y., C.-T. Liu, T. N. Lee, W. E. Johns, H. W. Li, and M. Koga, Sea surface slope as the estimator of the Kuroshio volume transport east of Taiwan, *Geophys. Res. Lett.*, *28*, 2461–2464, 2001.

Yuan, Y., K. Takano, Z. Pan, J. Su, K. Kawatate, S. Imawaki, H. Yu, J. Chen, J. Ichikawa, and S. Umatani, The Kuroshio in the east China Sea and the currents east of the Ryukyu Islands during autumn 1991, *Mer*, *32*, 235–244, 1994.

Yuan, Y., A. Kaneko, J. Su, X. Ahu, Y. Liu, N. Gohda, and H. Chen, The Kuroshio east of Taiwan and in the East China Sea and the currents east of Ryukyu Islands during early summer of 1996, *J. Oceanogr.*, *54*, 217–226, 1998.

Zhang, D., W. E. Johns, T. N. Lee, C.-T. Liu, and R. Zantopp, The Kuroshio east of Taiwan: Modes of variability and relationship to interior meso-scale eddies, *J. Phys. Oceanogr.*, *31*, 1054–1074, 2001.

W. E. Johns, T. N. Lee, R. Zantopp, and D. Zhang, Rosenstiel School of Marine and Atmospheric Science, University of Miami, 4600 Rickenbacker Causeway, Miami, FL 33149, USA. (tlee@rsmas.miami.edu).

C.-T. Liu and Y. Yang, Institute of Oceanography, National Taiwan University, Taipei, Taiwan 106.

(Received July 10, 2000; revised May 29, 2001;
accepted June 14, 2001.)